Published in final edited form as:

Epilepsia. 2020 February ; 61(2): 287–296. doi:10.1111/epi.16433.

7 Tesla susceptibility-weighted analysis of hippocampal venous structures: Application to MR-normal focal epilepsy

Rebecca Emily Feldman[*,1,2,3], **Lara Vanessa Marcuse**[5], **Gaurav Verma**[2,3], **Stephanie Sian Gabriella Brown**[4], **Alexandru Rus**[2], **John Watson Rutland**[2], **Bradley Neil Delman**[2,3], **Priti Balchandani**[+,2,3], **Madeline Cara Fields**[+,5]

[1]Department of Computer Science, Math, Physics, and Statistics, University of British Columbia, Kelowna, British Columbia, Canada

[2]Translational and Molecular Imaging Institute, Icahn School of Medicine at Mount Sinai, New York, New York, USA

[3]Radiology, Icahn School of Medicine at Mount Sinai, New York, New York, USA

[4]Department of Psychiatry, University of Cambridge, Cambridge, UK

[5]Department of Neurology, Mount Sinai Hospital, New York, New York, USA

Abstract

Objective: Vascular structures may play a significant role in epileptic pathology. Although previous attempts to characterize vasculature relative to epileptogenic zones and hippocampal sclerosis have been inconsistent, an *in vivo* method of analysis would assist in resolving these inconsistencies and facilitate a comparison against healthy controls in a human model. Magnetic resonance imaging is a non-invasive technique which provides excellent soft tissue contrast, and the relatively recent development of susceptibility-weighted imaging has dramatically improved the visibility of small veins.

Methods: We built and tested a Hessian-based segmentation technique, which takes advantage of the increased signal and contrast available at 7 Tesla (7T) to detect venous structures *in vivo*. We

[*]Corresponding Author: rebecca.feldman@ubc.ca.
[+]Senior Authors

Declarations of Interest

Dr. Priti Balchandani is a named inventor on patents relating to magnetic resonance imaging (MRI) and RF pulse design. The patents have been licensed to GE Healthcare, Siemens AG, and Philips international. Dr. Balchandani receives royalty payments relating to these patents.

Dr. Balchandani is a named inventor on patents relating to Slice-selective adiabatic magnetization T2-preparation (SAMPA) for efficient T2-weighted imaging at ultrahigh field strengths, Methods for Producing a Semi-Adiabatic Spectral-Spatial Spectroscopic Imaging Sequence and Devices There of, and Semi-Adiabatic Spectral-spatial Spectroscopic Imaging. These patents have been filed through MSIP; they remain unlicensed, there is no discussion to license them in the near future, and there are consequently no royalties revolving around them.

Dr. Feldman is a named inventor on patents relating to magnetic resonance imaging (MRI) and RF pulse design, Semi-Adiabatic Spectral Spatial Spectrospatial Imaging (SASSI) and Semi-Adiabatic Matched Phase Spin Echo Power Independent of the Number of Pulses (SEAMS PINS). She does not receive financial compensation related to these patents.

The remaining authors report no conflict of interest concerning the materials or methods used in this study or the findings specified in this paper.

Ethical Publication Statement

We confirm that we have read the Journal's position on −issues involved in ethical publication and affirm that this report is consistent with those guidelines

investigate the ability of this technique to quantify vessels in the brain and apply it to an asymmetry analysis of vessel density in the hippocampus in patients with mesial temporal lobe epilepsy (MTLE) and neocortical epilepsy.

Results: Vessel density was highly symmetric in the hippocampus in controls (mean asymmetry = 0.080 ± 0.076, median = 0.05027), while average vessel density asymmetry was greater in neocortical (mean asymmetry = 0.23 ± 0.17, median = 0.14) and MTLE (mean asymmetry = 0.37 ± 0.46, median = 0.26) patients, with the decrease in vessel density ipsilateral to the suspected seizure onset zone. Post-hoc testing with 1-way ANOVA and Tukey's post-hoc test indicated significant differences in the group means ($p < 0.02$) between MTLE and the control group only.

Significance: Asymmetry in vessel density in the hippocampus is visible in patients with MTLE, even when qualitative and quantitative measures of hippocampal asymmetry show little volumetric differences between epilepsy patients and healthy controls.

Keywords

7T MRI; non-lesional focal epilepsy; temporal lobe epilepsy; SWI; hippocampus

Introduction

Epilepsy is a chronic condition that is characterized by recurrent seizures and actively affects approximately 1–8% of the worldwide population[1–5]. Mesial temporal lobe epilepsy (MTLE) is the most common seizure type in adult epilepsy. MTLE is often drug resistant and difficult to clinically manage. One of the most frequent magnetic resonance imaging (MRI) findings in adult MTLE is hippocampal sclerosis, which is characterized by gliosis and neuronal loss[6–9].

In vivo identification of hippocampal volume asymmetry or of a hyperintense lesion on structural MRI scans are both key indicators of hippocampal sclerosis. However, even patients without a clear lesion or volume asymmetry on pre-surgical imaging who do undergo successful surgery (guided by seizure semiology and both scalp and intracranial electroencephalography (EEG))) can have distinct, epileptogenic abnormalities identified in the resection via post-surgical histopathology[10, 11]. This suggests that there are discrete structural abnormalities that are not well characterized by current imaging protocols and analysis.

Vascular structures may play a significant role in epileptic pathology. In analysis of sclerotic hippocampi of temporal lobe epilepsy patients, changes in permeability of the blood-brain barrier have been reported[12–14]. Although previous attempts to characterize vasculature relative to epileptogenic zones and hippocampal sclerosis have been inconsistent, an increase in hippocampal vasculature, found through examination of immunohistochemistry markers such as collagen-IV and macroscopic observations of the epileptogenic zone, have been interpreted as evidence of an increase in hippocampal vasculature in MTLE[15–22]. However, this pattern is discordant with histochemical labeling studies employing alkaline phosphatase, a marker of endothelial cells in the blood-brain barrier and both high-magnification light- and electron- microscopy, which suggest a decrease of blood vessels

and visual identification of atrophic blood vessels in sclerotic hippocampi[23–26]. Existing techniques investigating alterations in vasculature during epilepsy have relied on *ex vivo* assessment of the resected hippocampus. An *in vivo* method would assist in resolving these inconsistencies and facilitate a comparison against healthy controls in a human model.

MRI is a non-invasive technique which provides excellent soft tissue contrast, and the relatively recent development of susceptibility-weighted imaging (SWI) has dramatically improved the visibility of small veins[27–29]. A number of algorithms making use of Hessian filters have been proposed to facilitate the segmentation of blood vessels made visible by SWI[15, 30–33]. In this work we build on the Steger algorithm[33] to create a Hessian-based segmentation technique, which takes advantage of the increased signal and contrast available at MRI strengths of 7 Tesla (7T) to detect venous structures *in vivo*. The method integrates high resolution SWI and anatomical knowledge derived from T1-weighted images. We investigate the ability of this technique to quantify vessels in the brain and apply it to an analysis of vessel density in the hippocampus in patients with neocortical epilepsy and MTLE.

Methods

Participants

Patients with epilepsy, between ages 18–78 years, were referred for 7T imaging by their epileptologist (M.C.F, L.V.M). Inclusion criteria for this analysis required epilepsy patients to 1) have suspected seizure onset in the temporal lobe (MTLE), *or* other forms of focal epilepsy from the neocortex, as revealed by their clinical history, seizure semiology and/or EEG data; 2) have standardized epilepsy protocol 1.5T or 3T MRI scans that were read as MRI-normal, i.e., without epileptogenic lesions; by a neuroradiologist (BND) and 3) have no contraindications to 7T MRI. Institutional Review Board approval for human research was obtained for this study and written, fully informed, consent was given by each participant prior to enrollment. A total of 17 MTLE patients (10 female; mean age = 37±15 years), underwent scanning for the present study, as well as 17 neocortical patients (10 female, age 37±13 years), selected for similar age and gender, and 17 age and gender matched normal controls (10 female, mean age = 37±13 years) (Table 1). All MTLE patients recruited to participate in 7T research on epilepsy patients with MRI-normal clinical scans were analyzed. Control volunteers were included if they had no contraindications to 7T MRI and self-identified with no history of seizure or epilepsy. From neocortical patients, seizure onset was suspected to be focal (10, including nine frontal and one parietal) or multi-focal (7). Additional clinical information is provided in the supplemental Tables e1 and e2.

Data acquisition

All imaging was performed on a 7T whole body scanner (Magnetom, Siemens Healthcare, Erlangen, Germany). A SC72CD gradient coil (max slew rate = 200T/m/s, G_{max} = 70 mT/m) was used with a single channel transmit and a 32-channel receive head coil (Nova Medical, Wilmington, MA, USA). The patients were scanned using a 90-minute epilepsy MRI protocol, and qualitative analysis of the data has been reported[34]. For this analysis we made use of the T1-weighted (MP2RAGE[35]) sequence (TA 7:26; voxel size 0.8 × 0.8 × 0.8

mm^3; FOV 255 × 183 mm^2; TR 6000 ms; TE 5.1 ms; TI1/TI2 1050/3000 ms; FA1/FA2 5/4; Matrix 282 × 146; BW 130 Hz/pixel; iPAT 3) and the SWI sequence (TA 7:30; voxel size 0.2 × 0.2 × 1.5 mm^3; TR 23 ms; TE 14 ms; FA 12; matrix 1024 × 832; BW 150 Hz/Pixel; iPAT 3).

Vessel tracing

The protocol developed to automatically detect potential venous structures from the acquired data is illustrated in Figure 1. Uniform Denoised (UNIDEN) images were produced from the MP2RAGE acquisitions (Figure 1A) and minimum intensity projection (mIP) images through 5 contiguous slices were produced from the magnitude of the SWI acquisition (Figure 1B). Masks were created using cortical, subcortical and white matter volumetric segmentation of the brain in FreeSurfer v6.0 (http://surfer.nmr.mgh.harvard.edu, MGH). The UNIDEN image and associated mask were co-registered to the SWI image using the SPM 12 software (www.fil.ion.ucl.ac.uk, Wellcome Center for Human Neuroimaging). The vessel tracing algorithm also utilized a volumetric segmentation of the hippocampus created in FreeSurfer (Figure 1D). The components of the segmentation comprising the hippocampus were combined to create a mask of the desired region of interest (ROI).

The mIP images were processed to detect potential venous structures based on Frangi and Steger[32, 33] methods for detection and segmentation implemented in Matlab (The Mathworks, Inc, Natick, MA). Vessel enhancement was performed by finding the eigenvalues of the Hessian matrix and extracting the principle direction[32]. The results were masked using the combined hippocampal segmentation to include only the ROI (Figure 1E). The resulting three-dimensional datasets were linked along an 18-connected network through the nearest neighbors. Individual objects were characterized using the '*bwlabel*' function in Matlab. Resultant networks excluded objects with a connected length of less than 4 voxels (Figure 1F). A consistent threshold was used for all analysis. The scripts used to produce this analysis are available upon reasonable request to the corresponding author.

Verification

The vessel tracing protocol was validated against manually traced vessels across 13 non-contiguous axial mIP slices of a control SWI image representing the brain from the basal ganglia to the vertex. The manual tracings were performed in Osirix Image analysis software (Pixmeno, Geneva). For comparison, the vessel tracing protocol was applied to the same slices, constrained by a mask containing a volumetric segmentation of white matter and gray matter. The manual and automatic vessel tracings were compared, and for the purposes of this analysis, the manual segmentations were defined to be the gold standard manual positive results (mP). The vessels detected on both the manual and automatic vessel tracing protocol were defined as true positive results (TP) and the venous structures detected on the manual segmentation but missed on the automatic tracing were defined as false negative results (FN). Finally, structures which were visible on the automatic tracing but absent from the manual tracing were defined as false positives based on the manual results (manual false positives, mFP) for the purpose of this calculation. True negatives (TN), regions which were not marked in both the manual segmentation and the automated segmentation, constituted the majority of the image but were not segmented into objects or quantified.

Sensitivity of the automatic object segmentation was calculated using Equation 1:

$$Sensitivity = \frac{TP}{TP + FN} \quad \text{Equation 1}$$

Positive predictive value (PPV) was calculated using Equation 2:

$$PPV = \frac{TP}{TP + FP} \quad \text{Equation 2}$$

Sensitivity and PPV were calculated for each slice, and for the overall set of 13 slices based on the manual segmentation gold standard.

To evaluate the manual markings used as our standard, we randomly selected 20% of the mFP identified through comparison of the manual and automatic tracings and evaluated the 6 slices surround the marking. The mFP was then classified as either *accurate segmentation* (i.e., an in-plane or through-plane visualization of a vessel that was missed by the manual segmentation and captured by the automatic segmentation) or a *false segmentation* (i.e., noise or other image feature not identifiable as a vessel that was captured by the automatic segmentation).

Finally, true positive voxels (TPv), true negative voxels (TNv), false positive voxels (FPv), and false negative voxels (FNv) were identified using a voxel-wise comparison of the manual and automatic segmentations. From these values a voxel-wise sensitivity, specificity, PPV, and the false positive rate (FPR) were calculated.

Vessel Density analysis of the hippocampus

Hippocampal volumes (HV) for each subject were the total volume of the voxels contained within the volumetric segmentation of the T1-weighted images. This was calculated by determining the total number of voxels contained within each segmentation and multiplying by the acquired voxel volume. The same volumetric segmentations were used as the mask to demarcate the ROI for the automatic vessel tracing. The vessel density (VD) on both the left and right was estimated by calculating vessel volume (VV) as the total number of voxels traced in each ROI scaled by the voxel volume and dividing by HV (Equation 3).

$$VD = \frac{VV}{HV} \quad \text{Equation 3}$$

To explore left/right asymmetry, an asymmetry index (AI) (Equation 4) and absolute asymmetry index (|AI|)(Equation 5) were calculated for both HV (AI_v) and VD (AI_D). For the calculation of AI_v and $AI_{D,}$ R represents HV or VD in the right ROI and L represents HV or VD in the left ROI.

$$AI = \frac{(R - L)}{\frac{1}{2}(R + L)} \quad \text{Equation 4}$$

$$|AI| = \frac{|(R-L)|}{\frac{1}{2}(R+L)} \quad \text{Equation 5}$$

To explore the correlation between HV and VD, HV and VD were calculated over the total hippocampus (left and right) for each subject and the Pearson product moment correlation coefficient was calculated for each group (MTLE, neocortical, and control) and for the combined population of epilepsy patients (MTLE and neocortical).

Statistical analysis

The hippocampal volumes and vessel densities in the right and left hemisphere amongst MTLE, neocortical, and controls were calculated. Patients and controls were compared using both $|AI_V|$ and $|AI_D|$ and between group differences were calculated using a one-way ANOVA and Tukey's post-hoc test.

Results

Tracing verification

The SWI mIP (Figure 2A and 2B) served as the substrate for both the manual tracing (Figure 2C and 2D) and the automated tracing (Figure 2E and 2F). The validation set contained a total of 1245 manually traced vessels used as the gold standard and 1444 veins were identified by the automated method. 1215 veins were concordant between the two methods. A total of 229 objects were labeled as veins by the automated method where none were indicated in the manual tracing (mFP). A total of 30 veins were only seen by manual tracing. The sensitivity of the automated tracing technique, calculated using Equation 1, is plotted in Figure 3A and ranged between 0.81 and 1.0, while PPV of the method ranged between 0.63 and 1.00. Summary statistics give a sensitivity of 0.98 and a PPV of 0.84 (Figure 3B).

Analysis of False Positives

Of the mFPs reexamined (approximately 20% of the 229 of the mFPs), 3/46 (6.5%) objects were classified as *false segmentations*, and the remaining 43/46 (93.5%) were classified as *accurate segmentations* (an example Figure 2). Of the *accurate segmentations*, 27/43 (62.8%) were fully visible in the plane of the image, 13/43 (30.2%) were partially visible in the plane of the image but more fully visible in the slice immediately above or below the plane of the marked image, and 3/43 (7.0%) vessels running essentially perpendicular to the plane of the image, identified as points of susceptibility which persist through five or more slices.

Voxel-wise validation

A voxel-wise comparison between the manual and automatic tracings evaluated 6202326 voxels located within the brain mask over the 13 slices. The sensitivity of the automated technique compared to the manual segmentation was found to be 0.89 (TPv = 1053405, FNv

= 131345), and the specificity was found to be 0.96 (TNv = 4805978, FPv = 211598). Thus, the PPV was 0.83, and the FDR was 0.04.

Comparison between MTLE, neocortical and controls

The total hippocampal volumes in MTLE (mean = 2.1 ± 0.5 cm^3), neocortical (mean = 2.4 ± 0.2 cm^3) and controls (mean = 2.7 ± 0.3 cm^3) ranged between 1.8 and 3.5 cm^3, with the lowest hippocampal volume found in a patient with left temporal epilepsy, and the largest in a control.

Individually calculated AI_v and AI_d are reported in the supplementary information (Tables e1 and e2). In aggregate, there was little asymmetry in the control population in total hippocampal volume (mean $|AI_v|$ = 0.065 ± 0.04, median = 0.06). Although the mean volume asymmetry was slightly higher than controls in both neocortical (mean $|AI_v|$ = 0.066 ± 0.06, median = 0.05) and MTLE ($|AI_v|$ = 0.135 ± 0.15, median = 0.05), the medians were slightly lower as shown in Figure 4. A 1-way ANOVA resulted in no significant differences between the group means.

Vessel density was also highly symmetric in controls (mean $|AI_d|$ = 0.080 ± 0.076, median = 0.050), while average vessel density asymmetry was greater in neocortical (mean $|AI_d|$ = 0.23 ± 0.17, median = 0.14) and MTLE (mean $|AI_d|$ = 0.37 ± 0.46, median = 0.26) patients. A 1-way ANOVA indicated significant differences in the group means ($p < 0.02$) and Tukey's post-hoc test indicated that this result was driven by a significant difference between MTLE and controls groups ($p < 0.05$) in vessel density asymmetry. No other significant differences were indicated.

In all cases the asymmetry reflected a lower vessel density in the hippocampus ipsilateral to the suspected seizure onset zone when compared to the contralateral hippocampus (Tables e1 and e2). This result is shown for a control and an epilepsy patient over several slices of the hippocampus in Figure 5.

Correlation between VD and HV

Weak, but not significant positive correlation between VD and HV was found in all groups. The correlation in the control group was $r(15) = 0.02$, $p = 0.93$; the correlation in the neocortical group was $r(15) = 0.20$, $p = 0.43$; the correlation in the MTLE group was $r(15) = 0.31$, $p = 0.21$. Over the combined group of epilepsy patients (neocortical and MTLE) there was a weak significant correlation between VD and HV $r(32) = 0.33$, $p = 0.04$.

Discussion

The present study utilized SWI to assess changes in hippocampal venous vasculature *in vivo* and results show a decrease in vessel density in the hippocampus in patients with MTLE who have non-lesional clinical MRI's.

Comparison between manual and automatic vessel tracings

Our analysis demonstrates a high level of agreement between the manual and automatic tracings. The method was less sensitive in slices in the more inferior brain, closer to the

paranasal sinuses and basal ganglia. The PPV of the automatic object segmentation against the manual tracing was increasingly accurate from the basal ganglia to the vertex. The net PPV was calculated to be 0.84, meaning approximately 1 out of 6 objects traced automatically were not identified as a vessel during the manual marking (mFP). An examination of 46 (20%) of the mFPs revealed that 3 (7%) of the vessels were *falsely segmented* by the algorithm. By applying the same *accurate segmentation* and *false segmentation* rates to the rest of the sample, the number of false positives (*false segmentations*) could be corrected to 15, while the number of true positives (TP's and *accurate segmentations*) could be corrected to 1429. Finally, the number of FN's would remain unaffected (30 total).

The voxel-wise analysis produced values for sensitivity and PPV which were lower than the object-based validation. In addition to the voxels contained in the 229 mFP objects identified by the algorithm (Figure 2D and 2F), the boundaries identified on the manual and automatic vessel segmentations are not identical, thus objects identified as mTP's on the automatic segmentation contain voxels which are TPv, FPv, and FNv – reducing the overall specificity and positive predictive value.

Although the majority of structures (and voxels) were common to both the automatic and manual vessel segmentation techniques, each protocol also uniquely identified a set of vessel structures. The object-based segmentation revealed that while manual segmentation was more accurate in regions near the sinuses or where low overall signal rendered SWI less reliable but where it was possible to manually interpret the image through noise. However, the automatic segmentation technique did not suffer from inconsistencies due to manual rater fatigue and was likely better able to combine information across multiple imaging planes to identify vessels across slices, particularly closer to the vertex.

Volume Asymmetry

Hippocampal asymmetry, rather than overall hippocampus volume, is a more common qualitative metric used in conjunction with hyperintensity on FLAIR images to radiologically identify hippocampal sclerosis[36]. An analysis of the quantitative volumetric AI_v in neocortical, MTLE, and controls reveals only minor, non-significant changes to mean asymmetry in both groups of epilepsy patients when compared to controls (Figure 4A). This analysis was performed on data acquired from patients whose prior clinical scans were interpreted as non-lesional, in whom no significant qualitative hippocampal asymmetry had been described. Thus, this result of minimal quantitative volumetric hippocampal asymmetry in patients with neocortical epilepsy and MTLE is consistent with the initial referral criteria.

Vessel Density Asymmetry

Quantitative vessel analysis using SWI mIPs in MTLE and neocortical epilepsy did reveal structural indicators of the presence of disease even in the absence of a qualitative identification of volumetric hippocampal sclerosis. A qualitative examination of the 7T structural images for the two MTLE patients with high AI (Figure 4, $|AI| = 1.27$ and 1.79, Table 1), revealed suggestions of hippocampal asymmetry and bilateral hippocampal sclerosis not visible in their clinical scans. This appears consistent with previous work

investigating the hippocampus, and in particular the CA1 subfield and the cornu ammonis as a whole, which indicates that in epilepsy these regions are particularly susceptible to deterioration[6–9]. In TLE, changes in permeability of the blood-brain barrier in the hippocampus have been reported, likely associated with the development of the inflammatory processes that induce glial hypertrophy, proliferation and neuronal death[12–14]. It therefore follows that changes to vascular structures may play a significant role in, or may result from, epileptic pathology.

The abnormal vasodynamics coupled with a reduction in functional vessels might further contribute to microscopic hypoxia and ictal neurodegeneration[37, 38]. Thus, ongoing seizures may eventually involve structures and vasculature in the hippocampus even when the region is not implicated as a primary epileptogenic zone. Patients without suspected seizure onset zones in the mesial temporal lobes (neocortical) showed a mean asymmetry (mean $|AI_d|$ = 0.23 ± 0.17) greater than controls (mean $|AI_d|$ = 0.08 ± 0.76), but the posthoc test did not indicate significance. Approximately half (9/17) of the neocortical patients had $|AI_d| > 0.13$, which more closely resembled MTLE patients ($|AI_d| > 0.13$ in 13/17 patients) than controls ($|AI_d| > 0.13$ in 2/17 patients). This suggests that in approximately half of the epilepsy patients without EEG or clinical symptoms indicating a mesial temporal seizure onset zone (neocortical), there may be some degree of hippocampal involvement.

Correlation between HV and VD—For all subjects the voxel-wise vessel segmentation was normalized by the HV to produce VD in order to minimize the correlation between the metrics. In controls, the correlation between HV and VD was very weak and non-significant. However, for epilepsy patients, a weak positive correlation was detected between HV and VD in both groups. This correlation did not achieve significance for the sample size. However, when the correlation between HV and VD was analyzed for all epilepsy patients (MTLE and neocortical), a weak, but significant correlation was identified. This suggests that, in the presence of pathology, both hippocampus volume and vessel density are decreased and that sclerotic tissue is drained by disproportionately fewer intact vessel.

Although differences in the symmetry of hippocampus volumes were not identified, the analysis may have been limited by the segmentation tool used. Freesurfer may not be capable of providing segmentations with sufficient accuracy and precision to detect real, but small, alterations in hippocampus volumes in the 7T data sets evaluated here.

Future work evaluating a larger sample size with more precise segmentation tools could explore the correlation between VD and HV and indicate where a decrease in VD may identify hippocampal pathology before changes in HV are detected.

Hippocampal vasculature in previous ex vivo work

Although histochemical markers of increased vessel formation would seem to be in conflict with our finding of reduced vessel density ipsilateral to the suspected epileptogenic zone[15], other *ex vivo* experiments have shown diminished histochemical labeling of alkaline phosphatase (AP) in CA1 subfields that exhibit sclerosis[23]. AP is a marker of endothelial cells in the blood-brain barrier, so gross reduction is a marker of lower concentrations of AP-positive vessels. Additionally, since AP activity appears to be altered during induced seizure

activity in rats, abnormalities in the AP genetic structure may prompt epileptic activity through perturbation of the role of AP to regulate GABA synthesis leading to alterations in GABAergic regulation[23, 24]. High magnification light and electron microscopy of resected specimens also suggests that blood vessels are diminished within epileptogenic zones within human hippocampi. Collectively, these findings appear to suggest that prior *ex vivo* results showing increased vascular markers have identified not only functional vessels providing drainage but also collapsed and atrophic vessel fragments in the labeling. When such vessel damage was taken into account, active vasculature was actually significantly reduced in sclerotic hippocampi[25, 26].

The presence of atrophic blood vessels in sclerotic hippocampi suggests that a reduction of 'normal' vasculature in this region is a characteristic of MTLE. This local reduction in functional veins may be representative of aberrant vasogenesis and is consistent with our imaging results identifying a decrease in structures carrying deoxygenated blood in the hippocampus. However, more imaging studies with larger sample sizes and validation with resected tissue will be necessary to truly ascertain the pathophysiological processes underlying these vascular differences.

Additional Limitations and future directions

SWI emphasizes the incoherent signals in each voxel and the phase accumulation due to local sources of magnetic susceptibility, leading to a magnification of the effect of small veins in the image[28]. Thus, we would expect an overemphasis on small vessels as detected by both the manual and automatic tracing methods.

Another limitation of the technique is the potential conflation of veins with other sources of T2*-shortening. In the validation set, approximately 3 of the 46 'false positives' identified through comparison between the manual tracing and the automatic segmentation we considered to be 'false segmentations' – that is segmentations which, upon visual inspections of the image, were considered to unlikely to be vessels. Other Image features, such as calcifications, and hemosiderin appear dark on the SWI. The filters designed by Frangi and Steger were constructed to detect long edges, such as roads and vessels. Thus, when applied to calcification or hemosiderin, punctate sources of susceptibility will not be segmented. However, when the impact of these features on the image become long, thin, and more vessel-like, the segmentation tool will detect them.

The proximity of veins to other susceptible structures such as air and bone, including near the skull base may challenge the detection of small structures using this technique. This may be problematic when analyzing veins near low signal structures, leading to impaired detection accuracy in regions affected by both RF and main field inhomogeneity.

Previous work has shown volume loss in selective hippocampal subfields is correlated to epilepsy[39–41]. It has been shown that different parts of the hippocampus show different levels of resistance to disruption in perfusion, with the CA1 region known to be particularly sensitive, while CA2, and CA3 are thought to be particularly resistant[42]. Thus, it may be possible that this change in vessel density is also associated with particular hippocampal subfields. By acquiring high resolution SWI of sufficient quality to permit subfield

segmentation in addition to the vessel segmentation, it may be possible to further localize and characterize this change in subfield vasculature as it relates to MTLE.

Finally, only group differences in asymmetry were evaluated, due to the limited sample size. Future work, on a larger sample size would power a direct comparison of hippocampus volume and vessel density which could highlight bilateral pathology in both MTLE and neocortical epilepsy patients which is lost in the self-normalization intrinsic to the AI calculation. The analysis of vessel density symmetry in patients with neocotical epilepsy did not yield results significantly different from that of controls. There was a wider distribution of asymmetry in neocortical patients when compared to controls. High vessel density asymmetry among neocortical patients may implicate a wider seizure network. Future work could include a larger patient population, seizure duration, seizure severity and an analysis of refractoriness alongside vessel density asymmetry in the hippocampus and possibly throughout the brain. Further validation of vessel density asymmetry as a biomarker through imaging and histology may help to provide a means of identifying patients who are more likely to be refractory to medications, help to target electrode placement surgically during intracranial monitoring to evaluate more elaborate seizure networks as well as to guide interventions such as responsive neurostimulator placement.

This experiment aggregates vessel density over the entire hippocampus. Measurement of this metric as part of a comprehensive epilepsy imaging protocol may permit us to follow and assess structural changes associated with MTLE and eventually prevent or ameliorate the progression of neuronal damage in patients via the administration of targeted pharmacotherapy[38].

Conclusions

We introduce and validate a novel method of venous structure detection and report *in vivo* evidence of reduced functional vasculature in the hippocampus associated with MTLE. This feature is visible in patients with MTLE, even when qualitative and quantitative measures of hippocampal asymmetry show little volumetric differences between epilepsy patients and controls.

Supplementary Material

Refer to Web version on PubMed Central for supplementary material.

Acknowledgements

The research reported in the manuscript was supported by NIH-NINDS R00 NS070821; NIH R01 MH109544; DOD W81XWH-18-ERP-IDA

References

1. Ngugi AK, Bottomley C, Kleinschmidt I, Wagner RG, Kakooza-Mwesige A, Ae-Ngibise K, et al. Prevalence of active convulsive epilepsy in sub-Saharan Africa and associated risk factors: cross-sectional and case-control studies. Lancet Neurol 2013;12:253–263. [PubMed: 23375964]
2. Bell GS, Sander JW. The epidemiology of epilepsy: the size of the problem. Seizure 2001;10:306–314. [PubMed: 11466029]

3. Murray CJ, Vos T, Lozano R, Naghavi M, Flaxman AD, Michaud C, et al. Disability-adjusted life years (DALYs) for 291 diseases and injuries in 21 regions, 1990–2010: a systematic analysis for the Global Burden of Disease Study 2010. Lancet 2012; 380:2197–2223. [PubMed: 23245608]

4. WHO. Epilepsy:epidemiology, aetiology and prognosis. Geneva: World Health Organization, 2001.

5. Belhocine M, deBoer H, Mandlhate C. Epilepsy in the WHO African Region: Bridging the Gap. Geneva: World Health Organization, 2004.

6. Crespel A, Coubes P, Rousset MC, Alonso G, Bockaert J, Baldy-Moulinier M, et al. Immature-like astrocytes are associated with dentate granule cell migration in human temporal lobe epilepsy. Neurosci Lett 2002;330:114–118. [PubMed: 12213646]

7. Crespel A, Rigau V, Coubes P, Rousset MC, de Bock F, Okano H, et al. Increased number of neural progenitors in human temporal lobe epilepsy. Neurobiol Dis 2005; 19:436–450. [PubMed: 16023586]

8. Rigau V, Morin M, Rousset MC, de Bock F, Lebrun A, Coubes P, et al. Angiogenesis is associated with blood-brain barrier permeability in temporal lobe epilepsy. Brain 2007; 130:1942–1956. [PubMed: 17533168]

9. Meldrum B, Bruton C. Greenfield's Neuropathology In: Adams J, Duchen L, editors. Greenfield's Neuropathology. 5th Edition ed. London 1992 p. 1246–1283.

10. Duncan JS, Sander JW, Sisodiya SM, Walker MC. Adult epilepsy. Lancet 2006; 367:1087–1100. [PubMed: 16581409]

11. So EL. Role of neuroimaging in the management of seizure disorders. Mayo Clin Proc 2002;77:1251–1264. [PubMed: 12440562]

12. Ravizza T, Gagliardi B, Noe F, Boer K, Aronica E, Vezzani A. Innate and adaptive immunity during epileptogenesis and spontaneous seizures: evidence from experimental models and human temporal lobe epilepsy. Neurobiol Dis 2008;29:142–160. [PubMed: 17931873]

13. Ravizza T, Noe F, Zardoni D, Vaghi V, Sifringer M, Vezzani A. Interleukin Converting Enzyme inhibition impairs kindling epileptogenesis in rats by blocking astrocytic IL-1beta production. Neurobiol Dis 2008; 31:327–333. [PubMed: 18632279]

14. Oby E, Caccia S, Vezzani A, Moeddel G, Hallene K, Guiso G, et al. In vitro responsiveness of human-drug-resistant tissue to antiepileptic drugs: insights into the mechanisms of pharmacoresistance. Brain Res 2006; 1086:201–213. [PubMed: 16631625]

15. Vigneau-Roy N, Bernier M, Descoteaux M, Whittingstall K. Regional variations in vascular density correlate with resting-state and task-evoked blood oxygen level-dependent signal amplitude. Hum Brain Mapp 2014;35:1906–1920. [PubMed: 23843266]

16. Leal-Campanario R, Alarcon-Martinez L, Rieiro H, Martinez-Conde S, Alarcon-Martinez T, Zhao X, et al. Abnormal Capillary Vasodynamics Contribute to Ictal Neurodegeneration in Epilepsy. Sci Rep; 7:43276. [PubMed: 28240297]

17. Pitkanen A, Lukasiuk K. Molecular and cellular basis of epileptogenesis in symptomatic epilepsy. Epilepsy Behav 2009;14 Suppl 1:16–25. [PubMed: 18835369]

18. Morin-Brureau M, Lebrun A, Rousset MC, Fagni L, Bockaert J, de Bock F, et al. Epileptiform activity induces vascular remodeling and zonula occludens 1 downregulation in organotypic hippocampal cultures: role of VEGF signaling pathways. J Neurosci 2011; 31:10677–10688. [PubMed: 21775611]

19. Morin-Brureau M, Rigau V, Lerner-Natoli M. Why and how to target angiogenesis in focal epilepsies. Epilepsia 2012; 53 Suppl 6:64–68. [PubMed: 23134498]

20. Penfield W, Jasper HH, McNaughton F. Epilepsy and the functional anatomy of the human brain: Churchill; 1954.

21. Haglund MM, Ojemann GA, Hochman DW. Optical imaging of epileptiform and functional activity in human cerebral cortex. Nature 1992; 358:668–671. [PubMed: 1495561]

22. Tae WS, Joo EY, Kim JH, Han SJ, Suh YL, Kim BT, et al. Cerebral perfusion changes in mesial temporal lobe epilepsy: SPM analysis of ictal and interictal SPECT. Neuroimage 2005; 24:101–110. [PubMed: 15588601]

23. Erakovic V, Zupan G, Varljen J, Laginja J, Simonic A. Altered activities of rat brain metabolic enzymes in electroconvulsive shock-induced seizures. Epilepsia 2001; 42:181–189. [PubMed: 11240587]

24. Fonta C, Negyessy L, Renaud L, Barone P. Areal and subcellular localization of the ubiquitous alkaline phosphatase in the primate cerebral cortex: evidence for a role in neurotransmission. Cereb Cortex 2004 6 14:595–609. [PubMed: 15054075]
25. Alonso-Nanclares L, DeFelipe J. Alterations of the microvascular network in the sclerotic hippocampus of patients with temporal lobe epilepsy. Epilepsy Behav 2014; 38:48–52. [PubMed: 24406303]
26. Kastanauskaite A, Alonso-Nanclares L, Blazquez-Llorca L, Pastor J, Sola RG, DeFelipe J. Alterations of the microvascular network in sclerotic hippocampi from patients with epilepsy. J Neuropathol Exp Neurol 2009; 68:939–950. [PubMed: 19606060]
27. Haacke E, Xu Y, Cheng Y, Reichenbach J. Susceptibility weighted imaging (SWI). Magn Reson Med 2004; 52:612–618. [PubMed: 15334582]
28. Liu S, Buch S, Chen Y, Choi HS, Dai Y, Habib C, et al. Susceptibility-weighted imaging: current status and future directions. NMR Biomed 2017; 30:e3552.
29. Reichenbach JR, Barth M, Haacke EM, Klarhofer M, Kaiser WA, Moser E. High-resolution MR venography at 3.0 Tesla. J Comput Assist Tomogr 2000; 24:949–957. [PubMed: 11105717]
30. Ward PGD, Ferris NJ, Raniga P, Dowe DL, Ng ACL, Barnes DG, et al. Combining images and anatomical knowledge to improve automated vein segmentation in MRI. Neuroimage 2017; 165:294–305. [PubMed: 29079523]
31. Lesage D, Angelini ED, Bloch I, Funka-Lea G. A review of 3D vessel lumen segmentation techniques: models, features and extraction schemes. Med Image Anal 2009;13:819–845. [PubMed: 19818675]
32. Frangi AF, Niessen WJ, Vincken KL, Viergever MA, editors. Multiscale vessel enhancement filtering. 1998; Berlin, Heidelberg: Springer Berlin Heidelberg.
33. Steger C. An Unbiased Detector of Curvilinear Structures. IEEE Transactions on Pattern Analysis and Machine Intelligence 1998;20:113–125.
34. RE F, Delman B, Pawha P, Dyvorne H, Rutland J, Yoo J, et al. 7T MRI in epilepsy patients with previously normal clinical MRI exams compared against healthy controls. PLOS One. 2019;14:e0213642. [PubMed: 30889199]
35. Marques JP, Kober T, Krueger G, van der Zwaag W, Van de Moortele PF, Gruetter R. MP2RAGE, a self bias-field corrected sequence for improved segmentation and T1-mapping at high field. Neuroimage 2010; 49:1271–1281. [PubMed: 19819338]
36. Ruber T, David B, Elger CE. MRI in epilepsy: clinical standard and evolution. Curr Opin Neurol 2018; 31:223–231. [PubMed: 29389747]
37. Marinkovic S, Milisavljevic M, Puskas L. Microvascular anatomy of the hippocampal formation. Surg Neurol 1992; 37:339–349. [PubMed: 1631758]
38. Farrell JS, Gaxiola-Valdez I, Wolff MD, David LS, Dika HI, Geeraert BL, et al. Postictal behavioural impairments are due to a severe prolonged hypoperfusion/hypoxia event that is COX-2 dependent. Elife 2016; 5:e193552.
39. Santyr BG, Goubran M, Lau JC, Kwan BYM, Salehi F, Lee DH, et al. Investigation of hippocampal substructures in focal temporal lobe epilepsy with and without hippocampal sclerosis at 7T. J Magn Reson Imaging 2017; 45:1359–1370. [PubMed: 27564217]
40. Peslova E, Marecek R, Shaw DJ, Kasparek T, Pail M, Brazdil M. Hippocampal involvement in nonpathological deja vu: Subfield vulnerability rather than temporal lobe epilepsy equivalent. Brain Behav 2019; 8:e00996.
41. Kreilkamp BAK, Weber B, Elkommos SB, Richardson MP, Keller SS. Hippocampal subfield segmentation in temporal lobe epilepsy: Relation to outcomes. Acta Neurol Scand 2018; 137:598–608. [PubMed: 29572865]
42. Duvernoy H. The human hippocampus: An atlas of applied anatomy. Munich: JF Bergmann Verlag; 1988.

Key Points

- Vessels were segmented in the hippocampus from high-resolution SWI images
- No significant difference in hippocampus symmetry was detected
- Significant changes in vessel symmetry in the hippocampus were detected in patients with mesial temporal lobe epilepsy

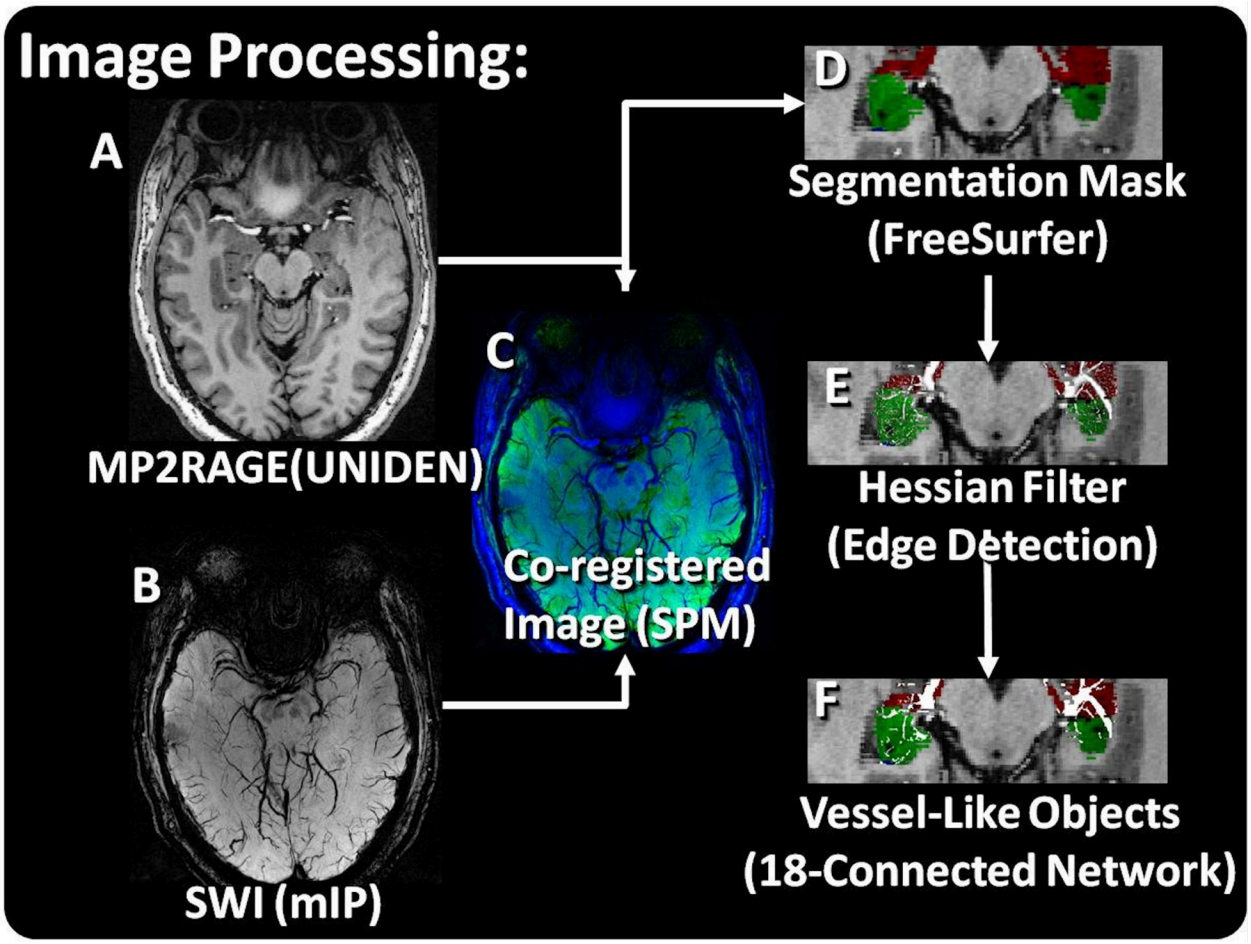

Figure 1:
Image Processing. A) The UNIDEN reconstruction of the MP2Rage image and B) the SWI mIP image were C) co-registered (MP2RAGE – green; SWI – blue). D) A segmentation of the hippocampus was used to mask the SWI with all components combined to make a right- and left- hippocampus mask. E) A Hessian edge detection filter was used to detect the ridges which were linked on F) an 18-connected network.

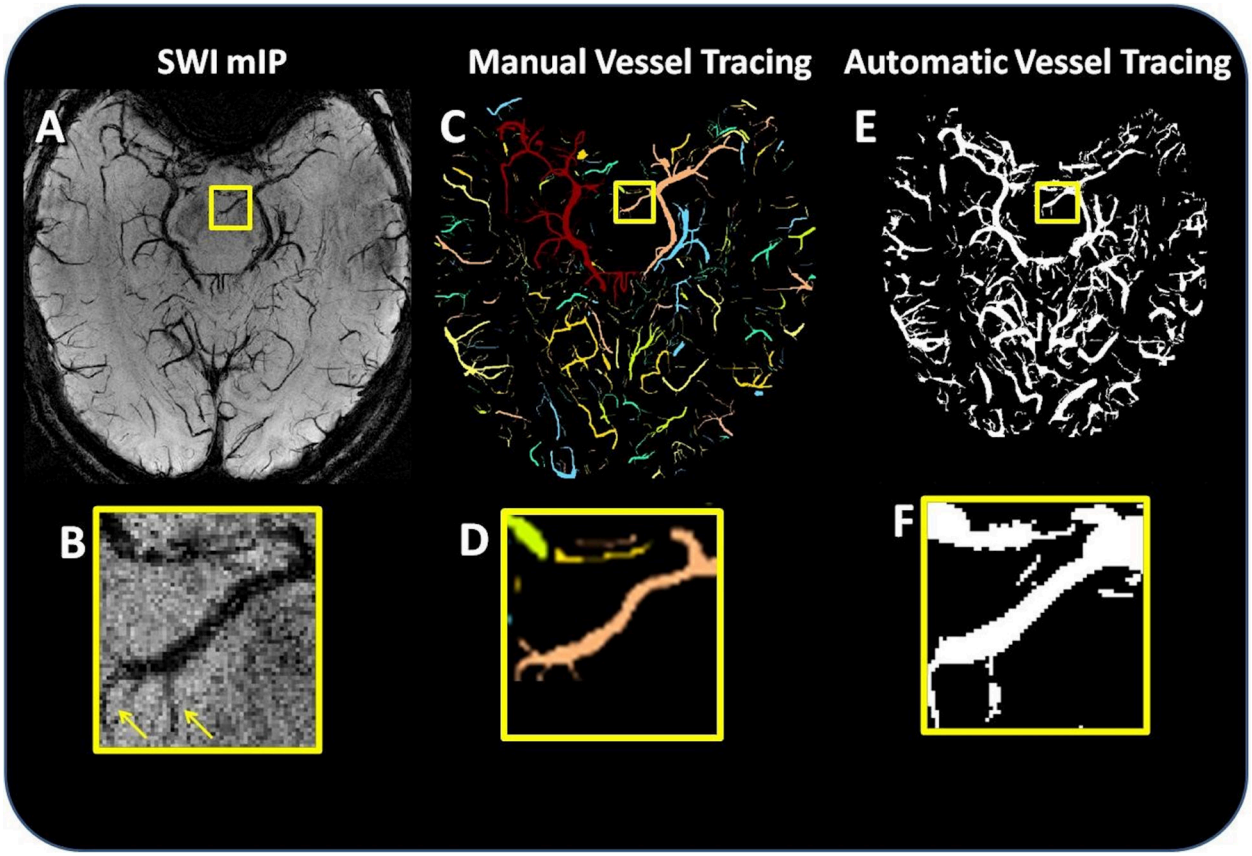

Figure 2:

Comparison of manual and automated segmentation. (A) Axial slice of the SWI mIP, and (B) a magnification of the mIP vessels highlighted in the yellow box. (C) Manually segmented vessels and (D) a magnification of the manual segmentation highlighted in the yellow box. (E) The result of automated vessel tracing, and (F) a magnification of the automatic segmentation highlighted in the yellow box. The arrows in (B) indicate that the automatic segmentation produced *accurate segmentations* of some mFP vessels (i.e., vessels which were identified in the automated segmentation but not in the manual segmentation).

A)

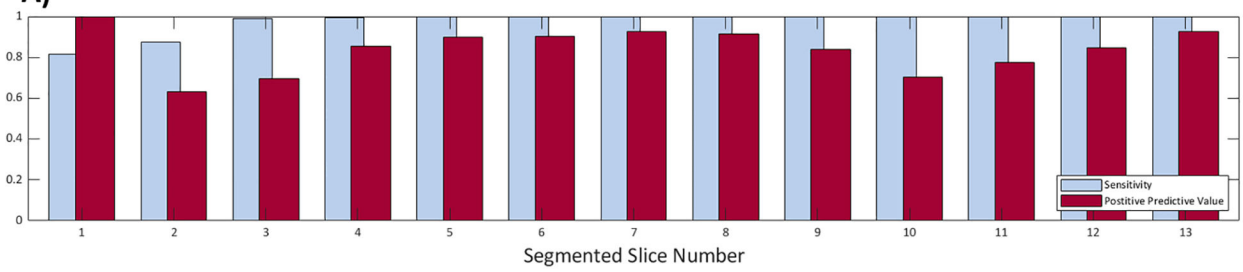

B)	# True Positive	# False Positive	# False Negative	Sensitivity	Positive Predictive Value
Overall	1215	229	30	0.98	0.84

Figure 3:

A) Slice-by-slice sensitivity and PPV calculation of the automated method against the manual gold standard. B) Overall sensitivity and PPV of automatic vessel tracing.

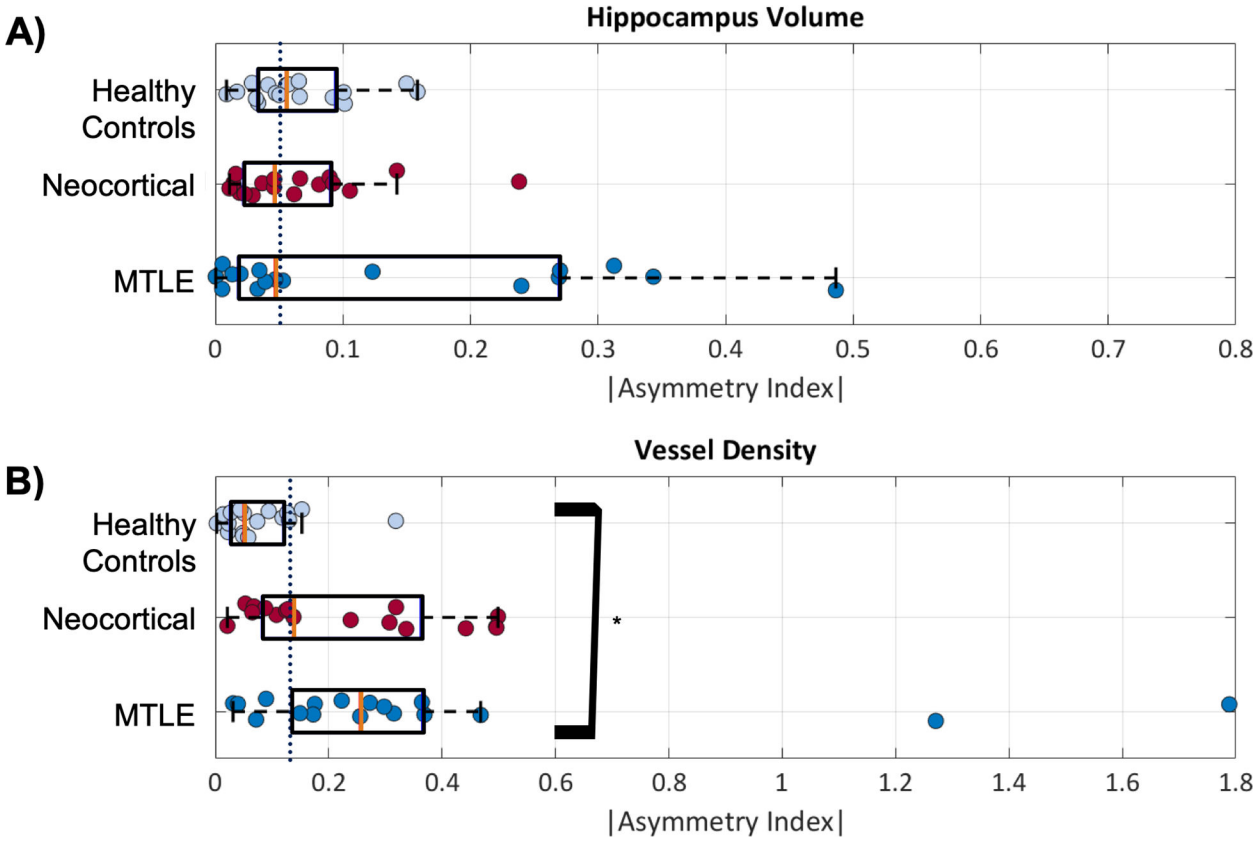

Figure 4:

Asymmetry of hippocampal volume and vessel density. The purple line in each figure represents the median value for all groups. A) The mean asymmetry of hippocampus volume is not significantly different between MTLE and neocortical patients and controls, although there is more variability in the epilepsy patients. B) The asymmetry in vessel density is significantly higher and MTLE than in controls (*) at $p < 0.04$. Median for each group is indicated with an orange bar.

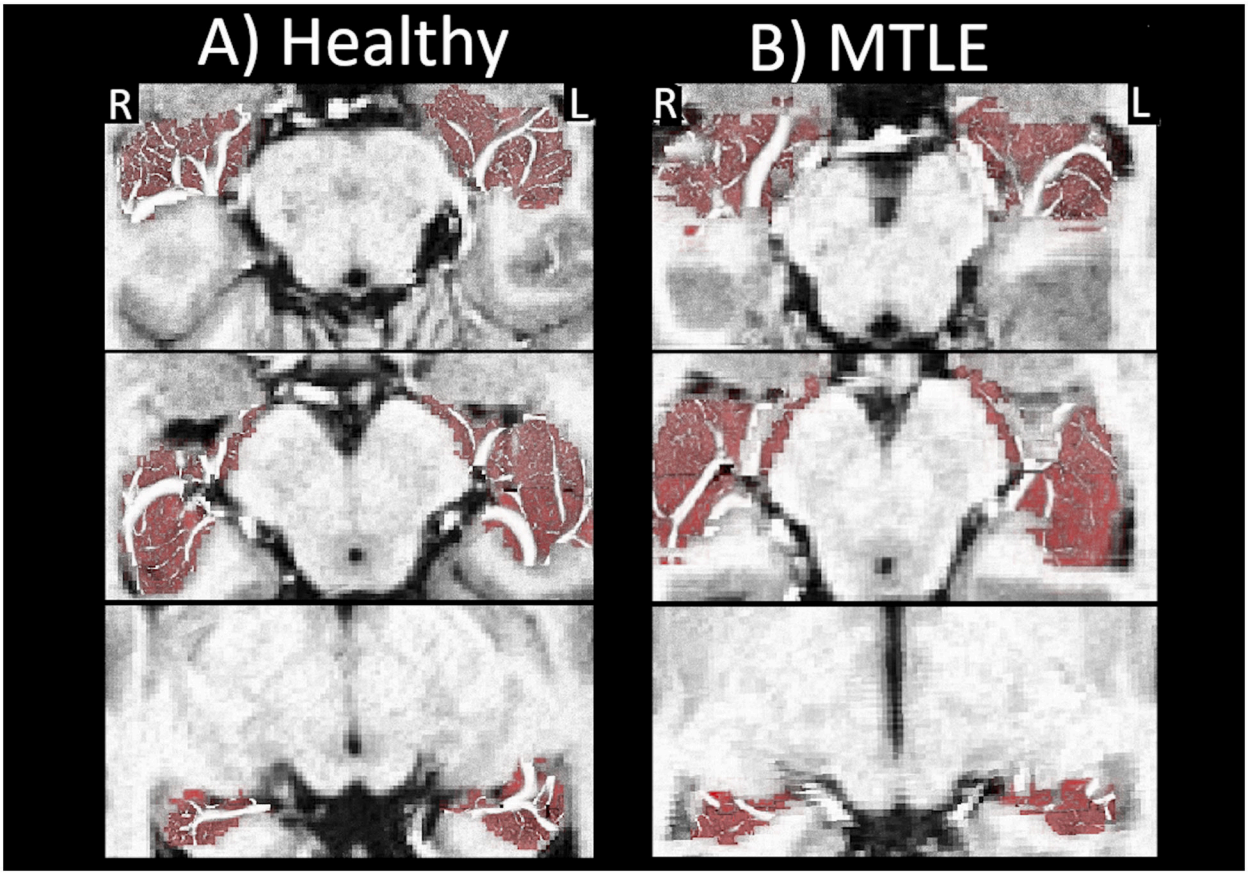

Figure 5:

Vessels in the hippocampus over 3 axial slices for A) a control and B) a patient with MTLE of suspected left onset. The radiological right hippocampus (R) is located on the left side of the image.

Table 1:

Participant Demographics

	MTLE	Neocortical	Healthy Controls
Number of Subjects	17	17	17
Male	7	7	7
Female	10	10	10
Age (Years ± STD)	37±15	37±13	37±13

Table of Participant Demographics. MTLE: Mesial Temporal Lobe Epilepsy; STD: Standard Deviation